

Lifetime predictions for virgin and recycled high-density polyethylene under creep conditions

A.D. Drozdov,^{*} R. Høj Jermiin, and J. deClaville Christiansen

Department of Materials and Production

Aalborg University

Fibigerstraede 16, Aalborg 9220, Denmark

Abstract

Recycling has become a predominant subject in industry and science due to a rising concern for the environment driven by high production volume of plastics. Replacement of virgin polymers with their recycled analogs is not always possible because recyclates cannot meet the same property profiles as their virgin counterparts. To avoid deterioration of the mechanical properties, it is proposed to replace a virgin polymer with a recycled polymer of another grade whose characteristics (measured in tensile tests) are close to those of the virgin material. This approach opens a way for the use of recycled polymers in short-term application, but its suitability for long-term applications has not yet been assessed. A thorough experimental investigation is conducted of the mechanical response of virgin high-density polyethylene (HDPE) used for insulation of pipes and recycled HDPE manufactured from post-consumer plastic waste (their stiffness, strength and elongation to break adopt similar values). A model is presented in viscoelastoplasticity of semicrystalline polymers. Its parameters are determined by matching experimental data in short-term relaxation and creep tests. The lifetime of virgin and recycled HDPE under creep conditions is evaluated by means of numerical simulation. It is shown that the stress–time to failure diagrams for virgin and recycled HDPE practically coincide.

Key-words: High-density polyethylene; Secondary recycling; Creep rupture; Lifetime assessment; Modeling.

1 Introduction

Although polymers have become an indispensable part of our life, an extreme increase in their production has led to a steadily growing proportion of plastic waste going into landfill.

^{*}E-mail: aleksey@m-tech.aau.dk

Due to considerable environmental concerns, recycling and reuse of polymers has become a predominant subject in industry and science [1, 2, 3].

Four approaches to recycling of plastic wastes are conventionally distinguished [4]:

1. At primary recycling, clean, uncontaminated, single-type waste with a controlled history is blended in-plant with virgin polymers.
2. At secondary recycling, plastic waste is sorted, separated from contaminants and other waste materials, cleaned, and compounded, before being mixed with virgin polymers.
3. Under tertiary recycling, solid plastic materials are converted into smaller molecules by means of chemical treatment. These intermediates are used as feed stocks for the production of new plastics.
4. The quaternary recycling consists in clean incineration (thermal and/or catalytic pyrolysis) to recover the energy content of plastic wastes.

This study focuses on the secondary recycling of high-density polyethylene (HDPE) and application of recycled HDPE for production of pipes. Due to degradation of post-consumer plastics during their service life and their thermo-mechanical degradation induced by recycling processes [5, 6], mechanical characteristics of recycled polymers, in particular, polyolefins, are lower than those of their virgin analogs [7]. Although deterioration of the mechanical properties observed in short-term tests on recycled HDPE is not very pronounced compared to the virgin polymer [8, 9, 10], it leads to a catastrophic reduction in the lifetime measured in long-term experiments. For example, the lifetime under creep conditions is reduced by one to two orders of magnitude [11, 12], the number of cycles to failure under fatigue conditions decreases by an order of magnitude [13, 14], and time to failure caused by crack propagation diminishes by one to three orders of magnitude [15, 16, 17].

To ensure comparable long-term properties of virgin and recycled plastics, it appears natural to replace a virgin HDPE with a recycled polymer (prepared from a different waste feedstock) whose mechanical properties after recycling are close to those of the virgin material. This approach has recently been proposed in [18, 19] where its environmental and economical advantages are discussed. The objective of this study is to demonstrate that HDPE samples manufactured from virgin and recycled polymers with similar mechanical characteristics (the Young modulus, yield stress, and strain at break) have practically identical lifetimes under creep conditions (which guarantees that they withstand 50 years of service life under tensile creep with the same stresses). This result is rather unexpected because creep resistance of solid polymers is determined to a large extent by their viscoelastic and viscoplastic properties (which differ noticeably for the virgin and recycled HDPE).

For the analysis, two grades of high-density polyethylenes were chosen: a virgin HDPE used for insulation of pipes for district heating and a recycled HDPE manufactured from post-consumer household plastic waste. The similarity of their mechanical responses was confirmed by observations in uniaxial tensile tests with a constant cross-head speed. A

thorough investigation of the viscoplastic and viscoplastic properties of these polymers was conducted in short-term tensile relaxation tests with various strains and creep tests with various stresses. Predictions of their lifetime in long-term uniaxial creep tests was performed with the help of the model recently developed in [20] and validated by comparison of observations in short-term tests with results of simulation.

The exposition is organized as follows. Experimental data on recycled HDPE in mechanical tests are reported in Section 2, where they are compared with observations on virgin HDPE presented in [20]. A brief description of the model in viscoelastoplasticity of semicrystalline polymers is provided in Section 3. Fitting of experimental data is conducted in Section 4.1. Validation of the model is performed in Section 4.2 where results of simulation are compared with observations. In Section 4.3, the stress–time to failure diagrams are discussed for virgin and recycled HDPE under tensile creep conditions. Concluding remarks are formulated in Section 5.

2 Materials and Methods

As a virgin material, we chose HDPE Borsafe HE3490-LS purchased from Borealis. It has density 959 kg/m^3 , melt flow rate 0.25 g/10 min , and melting temperature $130 \text{ }^\circ\text{C}$. For comparison, we used high-density polyethylene PEHD-R-E-GREY supplied by Aage Vestergaard Larsen A/S (Denmark). This polymer is manufactured from post-consumer household plastic waste, and it has density 960 kg/m^3 , melt flow rate 1.2 g/10 min , and melting temperature $130 \text{ }^\circ\text{C}$.

Dumbbell-shaped specimens (ISO 527-2-1B) with the total length 145 mm , the gauge length 65 mm , and the cross sectional area $9.81 \text{ mm} \times 3.95 \text{ mm}$ were prepared by using injection-moulding machine Ferromatik Milacron K110.

Uniaxial tensile tests were performed by means of the testing machine Instron 5568 equipped with an extensometer and a 5 kN load cell. Each test was repeated at least by twice.

Three series of tests were performed: (i) tensile tests with cross-head speeds $\dot{d} = 50 \text{ mm/min}$ up to breakage of samples, (ii) short-term stress relaxation tests (with the duration of 30 min) with strains ϵ ranging from 0.01 and 0.05 , and (iii) short-term creep tests (with the durations up to 6 h) with various stresses σ belonging to the interval between 9 and 20.5 MPa . All experiments were conducted at room temperature ($T = 21 \text{ }^\circ\text{C}$) in a climate-controlled room.

2.1 Tensile tests

Uniaxial tensile tests on virgin and recycled HDPE were conducted with cross-head speed $\dot{d} = 50$ (which corresponded to the strain rate $\dot{\epsilon} = 0.0088 \text{ s}^{-1}$) until breakage of samples. This cross-head speed is conventionally used for quality assessment of HDPE pipes under quasi-static loading [21]. The tests were repeated five times on samples of virgin HDPE and

six times on samples of recycled HDPE. The specimens were prepared by injection molding under the same conditions.

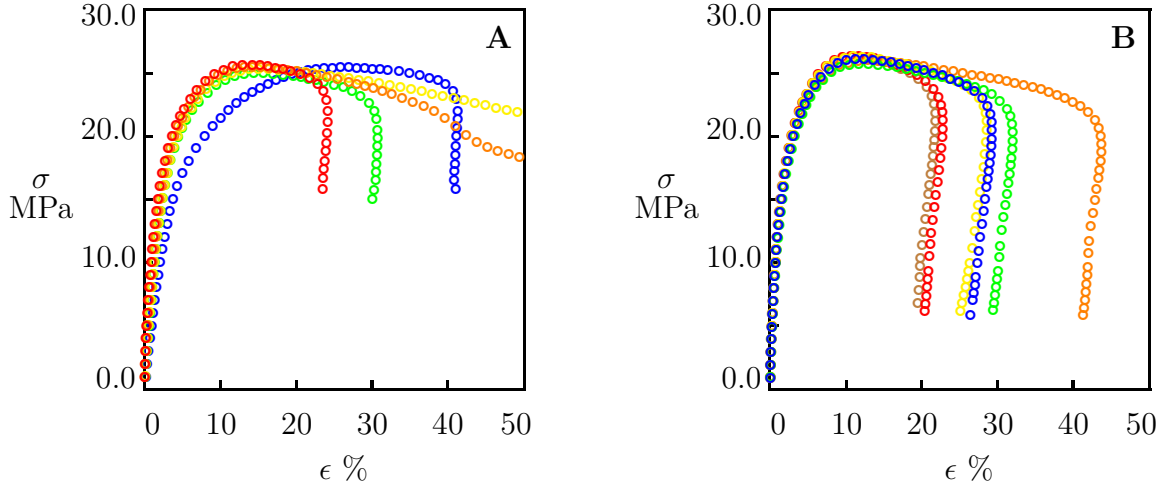


Figure 1: Tensile stress σ versus tensile strain ϵ . Circles: experimental data in tensile tests with strain rate 0.0088 s^{-1} on virgin (A) and recycled (B) HDPE.

Experimental data on virgin and recycled HDPE are depicted in Figure 1, where the engineering tensile stress σ is plotted versus the engineering strain ϵ . For both polymers under consideration, the stress σ increases with strain ϵ below the yield point ϵ_y , reaches its maximum (the yield stress σ_y) at ϵ_y , and decreases slightly afterwards. The strain at break ϵ_b is calculated as the maximum strain along the stress-strain diagram. Figure 1 reveals good repeatability and reliability of measurements. For example, the standard deviation δ_E of the Young's modulus E and the standard deviation δ_{σ_y} of the yield stress σ_y do not exceed 1% of their average values \bar{E} and $\bar{\sigma}_y$, respectively. The standard deviation δ_{ϵ_b} of the strain at break ϵ_b is relatively large, which may be explained by significant toughness of samples. The average values and the standard deviations of parameters E , σ_y and ϵ_b are collected in Table 1. This table shows that the stiffness (characterized by \bar{E}) of the recycled polymer exceeds that of the virgin HDPE by 35%, their strengths (estimated by $\bar{\sigma}_y$) coincide practically, whereas the toughness of the recycled HDPE (characterized by $\bar{\epsilon}_b$) is lower than that of virgin HDPE by 25%.

Table 1: Material parameters for virgin and recycled HDPE determined in tensile tests.

	\bar{E} GPa	δ_E GPa	$\bar{\sigma}_y$ MPa	δ_{σ_y} MPa	$\bar{\epsilon}_b$	δ_{ϵ_b}
Virgin	0.966	0.072	25.429	0.216	0.397	0.180
Recycled	1.305	0.014	26.166	0.224	0.297	0.073

2.2 Relaxation tests

Short-term stress relaxation tests on recycled HDPE were performed at strains $\epsilon_0 = 0.01$, 0.02 and 0.05. Tests were repeated by twice on different specimens manufactured under

the same conditions. In each test, a specimen was stretched with a cross-head speed of 50 mm/min up to the required strain ϵ_0 . Then, the strain was fixed, and the decay in stress σ was measured as a function of relaxation time $t_{\text{rel}} = t - t_0$, where t_0 stands for the instant when the strain ϵ reaches its ultimate value ϵ_0 .

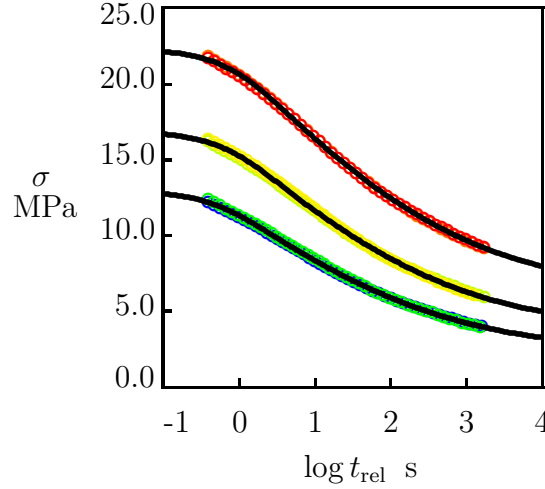


Figure 2: Tensile stress σ versus relaxation time t_{rel} . Circles: experimental data in relaxation tests with strains $\epsilon_0 = 0.01$ (blue and green), $\epsilon_0 = 0.02$ (lime and yellow), and $\epsilon_0 = 0.05$ (orange and red). Solid lines: results of numerical analysis.

Experimental data in relaxation tests on recycled HDPE are reported in Fig. 2 together with their fits by the model. In this figure, the engineering stress σ is plotted versus the logarithm ($\log = \log_{10}$) of relaxation time t_{rel} . Circles stand for the experimental data, and solid lines denote their fits by the model described in Section 3.

2.3 Creep tests

Two series of uniaxial creep tests on recycled HDPE were performed with “low” ($\sigma = 9.0, 10.0, 12.0$, and 14.5 MPa) and “high” ($\sigma = 17.5, 18.0, 19.0, 20.0$ and 20.5 MPa) tensile stresses. Each test was repeated by twice on specimens prepared under the same condition. In a creep test, a sample was stretched up to the required stress σ with a cross-head speed of 50 mm/min. Then, the stress was fixed, and an increase in tensile strain ϵ was measured as a function of creep time $t_{\text{cr}} = t - t_0$, where t_0 stands for the instant when the required stress σ is reached. The duration of creep tests with low stresses (6 h) was fixed. Creep tests with high stresses were conducted until breakage of samples.

Experimental data in creep tests on recycled HDPE are reported in Figures 3 (low stresses) and 4 (high stresses). In these figures, tensile strain ϵ is plotted versus creep time t_{cr} . For each stress σ , circles denote the mean (over observations on two samples) values of tensile strain, and the solid line stands for their approximation by the model described in Section 3.

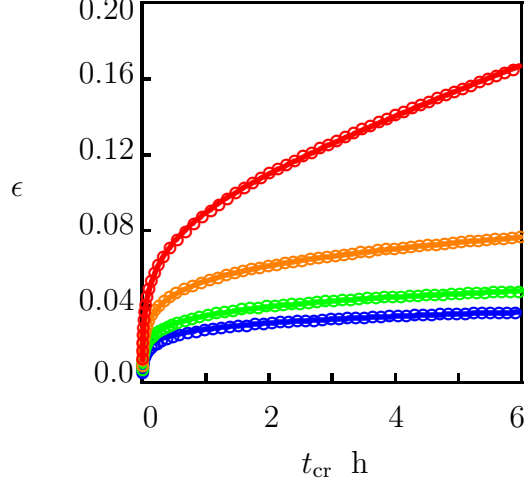


Figure 3: Tensile strain ϵ versus creep time t_{cr} . Circles: experimental data in creep tests with tensile stresses $\sigma = 9.0$ (blue), 10.0 (green), 12.0 (orange) and 14.5 (red) MPa. Solid lines: prediction of the model in viscoelastoplasticity.

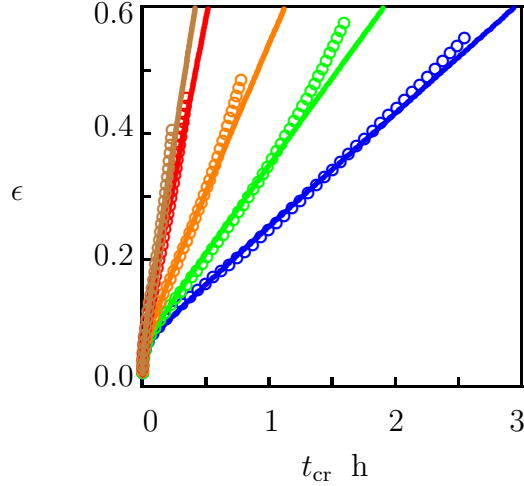


Figure 4: Tensile strain ϵ versus creep time t_{cr} . Circles: experimental data in creep tests with tensile stresses $\sigma = 17.5$ (blue), 18.0 (green), 19.0 (orange), 20.0 (red) and 20.5 (brown) MPa. Solid lines: prediction of the model in viscoelastoplasticity.

To assess the repeatability of measurements and the accuracy of their fitting, experimental data in creep tests with two highest stresses ($\sigma = 20.0$ and 20.5 MPa) are reported in Figure 5 together with results of numerical simulation. This figure reveals good reproducibility of observations. Figures 4 and 5 show that for all stresses under consideration, transition to the stage of tertiary creep (characterized by a rapid growth of tensile strain induced by damage of samples) occurs at the critical strain ϵ_* close to 0.4.

Experimental data in relaxation and creep tests on virgin HDPE are reported in [20]. Comparison of observations on virgin and recycled HDPE shows similarities of their time-

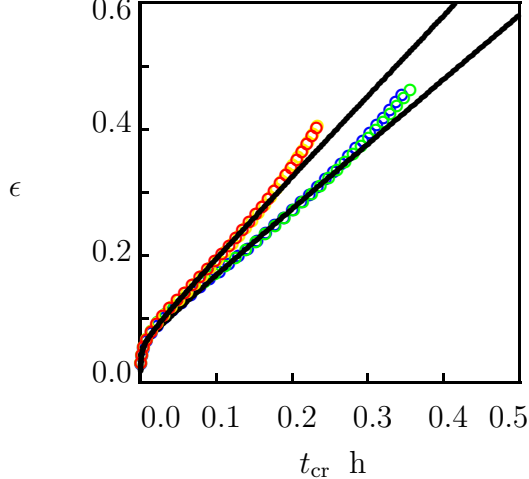


Figure 5: Tensile strain ϵ versus creep time t_{cr} . Circles: experimental data in creep tests with tensile stresses $\sigma = 20.0$ (blue, green) and $\sigma = 20.5$ (yellow, red) MPa. Solid lines: prediction of the model in viscoelastoplasticity.

dependent behavior. A detailed discussion of differences between their responses is provided in Section 4.

3 Model

The viscoelastoplastic response of HDPE under isothermal deformation with small strains is described by a constitutive model based on the following assumptions.

HDPE is a semicrystalline polymer consisting of two (amorphous and crystalline) phases (for simplicity, the presence of the rigid amorphous phase and inter-phases is disregarded [22]). The viscoplastic deformation of the amorphous phase describes (i) chain slip through the crystals, (ii) sliding of tie chains along and their detachment from lamellar blocks, and (iii) detachment of chain folds and loops from surfaces of crystal blocks [23]. The viscoplastic deformation in the crystalline phase reflects (i) inter-lamellar separation, (ii) rotation and twist of lamellae, and (iii) fine and coarse slip of lamellar blocks [24]. The viscoelastic response is associated with (i) relaxation of stresses in chains located in the amorphous regions and (ii) time-dependent decay in forces transmitted to the crystalline skeleton by tie chains [25].

A detailed account for the evolution of micro-structure in semicrystalline polymers under loading leads to a strong increase in the number of adjustable parameters. To make the model tractable, we treat HDPE as an equivalent non-affine network of polymer chains connected by permanent and temporary junctions [26]. The non-affinity of the network means that junctions between chains can slide with respect to their reference positions under deformation. Keeping in mind that the sliding process reflects viscoplastic deformations in the amorphous and crystalline regions, the strain tensor for plastic deformation ϵ_p consists

of two components

$$\epsilon_p = \epsilon_{pa} + \epsilon_{pc},$$

where the strain tensors ϵ_{pa} and ϵ_{pc} describe viscoplastic deformations in the amorphous phase and the crystalline skeleton, respectively. A similar decomposition of the plastic strain into two components was introduced in [27] to describe the viscoplastic deformation of semicrystalline polymers at finite strains.

Chains in the polymer network are bridged by permanent and temporary bonds. Both ends of a permanent chain are merged with the network by permanent bonds. At least one end of a temporary chain is connected with the network by a temporary (physical) bond that can break and reform. When both ends of a temporary chain are attached to the network, the chain is in its active state. When an end of an active chain separates from its junction at some instant τ_1 , the chain is transformed into the dangling state. When the free end of a dangling chain merges with the network at an instant $\tau_2 > \tau_1$, the chain returns into the active state. Attachment and detachment events occur at random times being driven by thermal fluctuations [28].

The network consist of meso-regions with various activation energies for breakage of temporary bonds. The rate of separation of an active chain from its junction in a meso-domain with activation energy u is governed by the Eyring equation

$$\Gamma = \gamma \exp\left(-\frac{u}{k_B T}\right),$$

where γ stands for the attempt rate, T is the absolute temperature, and k_B denotes the Boltzmann constant. For isothermal processes at a fixed temperature T , we introduce the dimensionless energy $v = u/(k_B T)$ and find that

$$\Gamma = \gamma \exp(-v). \quad (1)$$

Distribution of meso-domains with various activation energies v is described by the quasi-Gaussian formula

$$f(v) = f_0 \exp\left(-\frac{v^2}{2\Sigma^2}\right) \quad (v \geq 0), \quad (2)$$

where f stands for the distribution function. This function is characterized by the only parameter $\Sigma > 0$ that serves as a measure of inhomogeneity of a polymer network [25]. The pre-factor f_0 is determined from the normalization condition

$$\int_0^\infty f(v) dv = 1. \quad (3)$$

According to Equation (1), the average rate of rearrangement of temporary bonds in a transient network reads

$$\bar{\Gamma} = \gamma \int_0^\infty \exp(-v) f(v) dv. \quad (4)$$

Focusing on experimental data in uniaxial tests, we disregard volume deformation and treat of HDPE as an incompressible medium (according to [29, 30], the Poisson ratio of polyethylene ν belongs to the interval between 0.48 and 0.49).

Constitutive equations for a semicrystalline polymer under an arbitrary three-dimensional deformation with small strains were derived in [20] by means of the Clausius–Duhem inequality. Under uniaxial tensile relaxation with a fixed strain ϵ_0 , the governing relation reads

$$\sigma(t) = \sigma_0 \left[1 - \kappa \int_0^\infty f(v) \left(1 - \exp(-\Gamma(v)t) \right) dv \right], \quad (5)$$

where $\sigma(t)$ denotes tensile stress at an arbitrary instant $t \geq 0$,

$$\sigma_0 = E\epsilon_0 \quad (6)$$

stands for the stress at the initial instant $t = 0$, and κ denotes the ratio of the number of active chains to the total number of (active and permanent) chains per unit volume.

Given a strain ϵ_0 , Equations (5), (6) together with Equation (1) for $\Gamma(v)$ and Equation (2) for $f(v)$ involve four material parameters: (i) the Young’s modulus E , (ii) the rate of separation of active chains from their junctions γ , (iii) the measure of inhomogeneity of the equivalent network Σ , and (iv) the fraction of temporary bonds in the network κ . These quantities are found in Section 4 by matching experimental data on virgin and recycled HDPE.

Under uniaxial tensile creep with a fixed stress σ , the tensile strain ϵ is given by

$$\epsilon = \epsilon_e + \epsilon_{pa} + \epsilon_{pc}, \quad (7)$$

where ϵ_e stands for the strain caused by the viscoelastic response (rearrangement of temporary bonds between polymer chains in the network), and ϵ_{pa} , ϵ_{pc} are the strains induced by the viscoplastic flows (sliding of junctions between chains) in the amorphous and crystalline regions, respectively.

The strain $\epsilon_e(t)$ is determined by the formula

$$\epsilon_e(t) = \frac{\sigma}{E} + \kappa \int_0^\infty f(v) z(t, v) dv, \quad (8)$$

where the function $z(t, v)$ obeys the differential equation

$$\frac{\partial z}{\partial t} = \Gamma(v)(\epsilon_e - z), \quad z(0, v) = 0. \quad (9)$$

The viscoplastic flow in the amorphous phase is governed by the equation

$$\epsilon_{pa}(t) = A \left[1 - \exp(-\alpha \sqrt{t}) \right], \quad (10)$$

where A and α are adjustable parameters. The coefficient A stands for the maximum viscoplastic strain induced by sliding of junctions between chains, and α characterizes the rate of sliding of junctions with respect to their initial positions. An analog of Equation (10) (with \sqrt{t} replaced with t) is conventionally used to describe at the initial stage of flow of dislocations in crystalline materials [31].

The viscoplastic flow in the crystalline phase is described by the Norton equation [32]

$$\epsilon_{\text{pc}}(t) = Bt, \quad (11)$$

where B is an adjustable parameter.

Given a stress σ , the viscoplastic flow under creep conditions is determined by three material parameters: (i) the rate of sliding of junctions in the amorphous phase with respect to their initial positions α , (ii) the maximum viscoplastic strain A induced by sliding of junctions in the amorphous phase, and (iii) the rate of plastic flow in the crystalline phase B .

The influence of stress on the rate of sliding of junctions in amorphous regions α is described the power-law relation

$$\alpha = \alpha_0 \quad (\sigma < \sigma_*), \quad \alpha = \alpha_0 + \alpha_1(\sigma - \sigma_*)^m, \quad (12)$$

where α_0 , α_1 and m are material parameters, and σ_* denotes the threshold stress below which the viscoplastic flow is not observed.

The effect of stress σ on the coefficient A is determined by the formula

$$A = \frac{A_1}{1 + \exp[a(\sigma - \sigma_*)]} + A_2, \quad (13)$$

where A_1 , A_2 and a are material parameters. Equation (13) implies that A adopts different values $A_1 + A_2$ and A_2 far below and far above some threshold stress σ_* . Transition from the limiting values occurs in the close vicinity of σ_* only. The rate of transition is characterized by the coefficient a .

The influence of stress σ on the rate of viscoplastic flow in the crystalline phase B is governed by the equation

$$B = 0 \quad (\sigma < \sigma_*), \quad B = B_1(\sigma - \sigma_*)^n \quad (\sigma \geq \sigma_*), \quad (14)$$

where B_1 and n are adjustable parameters. The coefficient σ_* denotes the threshold stress below which the viscoplastic flow in spherulites does not occur.

Equations (12) and (14) imply that sliding of junctions is weakly affected by tensile stresses when these stresses remain relatively small, but the rate of sliding increases pronouncedly when σ exceeds its threshold value σ_* .

4 Results and Discussion

4.1 Fitting of experimental data

Material parameters for recycled HDPE are determined by matching observations presented in Figures 2 to 4.

4.1.1 Relaxation tests

We begin with the analysis of experimental data in relaxation tests. Each set of data in Figure 2 is fitted separately by means of Equation (5), where $\Gamma(v)$ is given by Equation (1), $f(v)$ is determined by Equation (2), and σ_0 is found from Equation (6). Given γ and Σ , the coefficients σ_0 and κ in Equation (5) are calculated by using the least-squares technique. The parameters γ and Σ are determined by the nonlinear regression method from the condition of minimum for the expression

$$\sum_k \left[\sigma_{\text{exp}}(t_k) - \sigma_{\text{sim}}(t_k) \right]^2,$$

where summation is performed over all instants t_k at which the data are reported, σ_{exp} denotes the tensile stress measured in the corresponding relaxation test, and σ_{sim} is given by Equation (5).

Table 2: Material parameters for recycled HDPE (relaxation tests with various strains ϵ_0)

ϵ_0	σ_0 MPa	γ s	Σ	κ
0.01	12.99	1.5	5.6	0.810
0.02	16.91	1.1	5.6	0.770
0.05	22.37	0.9	5.7	0.711

Figure 2 demonstrates good agreement between the experimental data in relaxation tests and their approximation of the model with the material constants collected in Table 2. This table shows that the coefficients γ , Σ and κ are weakly affected by tensile strain ϵ_0 (γ and κ are reduced slightly with ϵ_0 , whereas Σ remains practically constant). In what follows, changes in these coefficients with ϵ_0 are disregarded. Taking the value σ_0 at $\epsilon_0 = 0.01$ from Table 2 and using Equation (6), we calculate the Young's modulus $E = 1.299$ GPa. This value is very close to the value $\bar{E} = 1.305$ GPa found by approximation of the stress-strain curves under tensile deformation (Figure 1) and reported in Table 1.

Fitting observations in relaxation tests on virgin HDPE was performed in [20]. For comparison, the best-fit values of E , γ , Σ , and κ for virgin and recycled HDPE are collected in Table 3.

Table 3: Material parameters for virgin and recycled HDPE (relaxation tests with strain $\epsilon_0 = 0.01$)

HDPE	E GPa	γ s	Σ	κ
Virgin	0.947	2.1	7.2	0.862
Recycled	1.299	1.5	5.6	0.810

Table 3 shows that all parameters characterizing the linear viscoelastic behavior of virgin and recycled HDPE adopt similar values. The Young's modulus E of the recycled HDPE is higher (by 37%), whereas its attempt rate γ , measure of inhomogeneity of the temporary network Σ , and fraction of temporary junctions in the network κ are lower (by 29, 22, and 6 %, respectively). This difference may be explained by a higher degree of crystallinity of the recycled HDPE [33, 34], as well as a higher degree of long-chain branching in this polymer caused by its degradation under in-service conditions and recycling [35]. The average rates of rearrangement of temporary bonds $\bar{\Gamma}$ (determined by Equation (4)) coincide practically for virgin and recycled HDPE and read $\bar{\Gamma} = 0.255$ and $\bar{\Gamma} = 0.231 \text{ s}^{-1}$, respectively.

4.1.2 Creep tests

We now approximate the experimental creep diagrams on recycled HDPE depicted in Figures 3 to 5. Each set of data is matched separately by using the following algorithm.

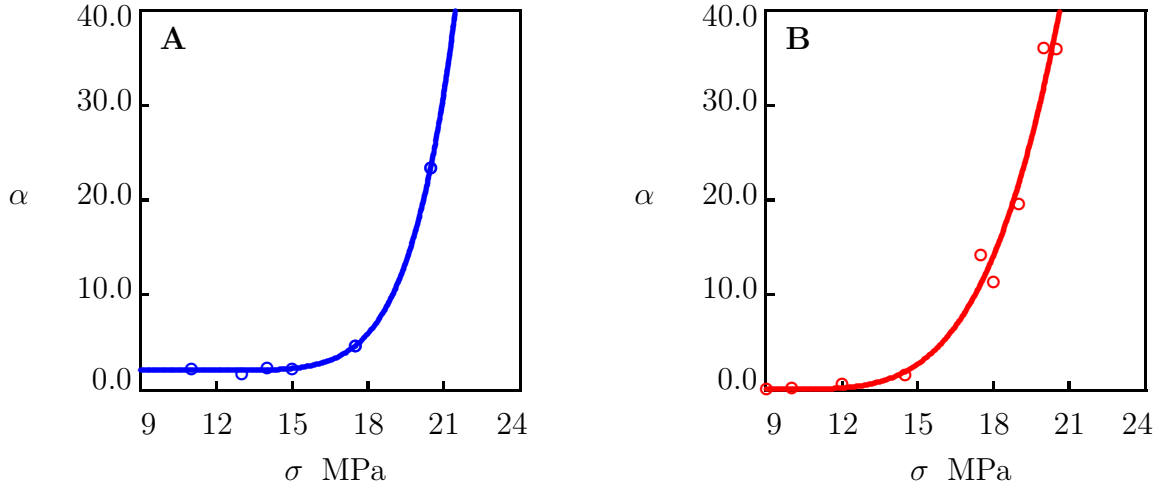


Figure 6: Parameter α versus tensile stress σ . Circles: treatment of experimental data on virgin (A) and recycled (B) HDPE. Solid lines: results of numerical analysis.

Given a stress σ , the viscoelastic strain ϵ_e is determined from Equations (8) and (9). These equations are integrated numerically by the Runge–Kutta method with the material parameters reported in Table 3. Afterwards, the viscoplastic strain $\epsilon_p = \epsilon_{pa} + \epsilon_{pc}$ is determined from Equations (10) and (11). Given α , the coefficients A and B are found by the least-squares technique. The parameter α is calculated by the nonlinear regression method from the condition of minimum for the expression

$$\sum_k \left[\epsilon_{p \text{ exp}}(t_k) - \epsilon_{p \text{ sim}}(t_k) \right]^2,$$

where summation is performed over all instants t_k at which the data are reported, $\epsilon_{p \text{ exp}}$ is determined from Equation (7), and $\epsilon_{p \text{ sim}}$ is found from Equations (10) and (11).

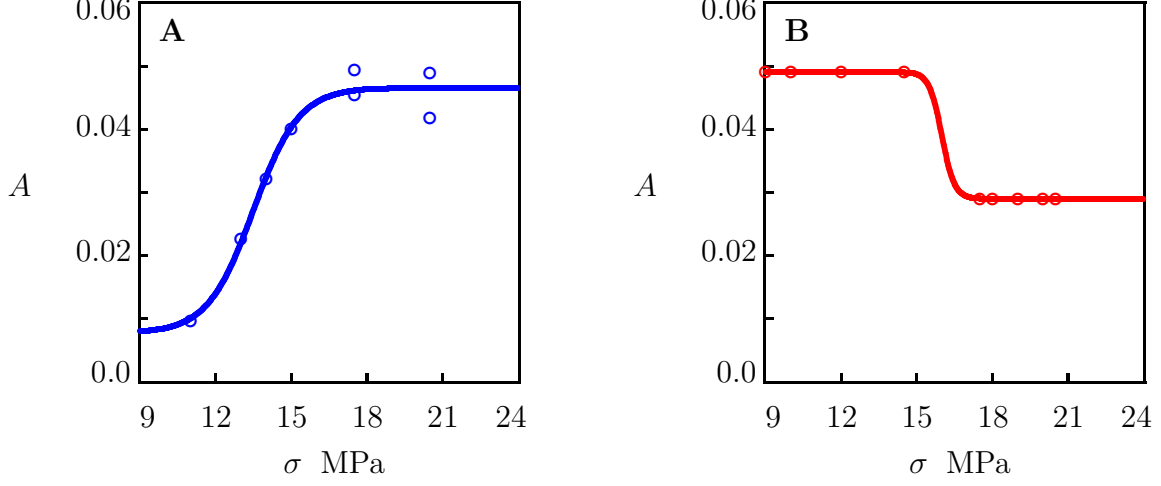


Figure 7: Parameter A versus tensile stress σ . Circles: treatment of experimental data on virgin (A) and recycled (B) HDPE. Solid lines: results of numerical analysis.

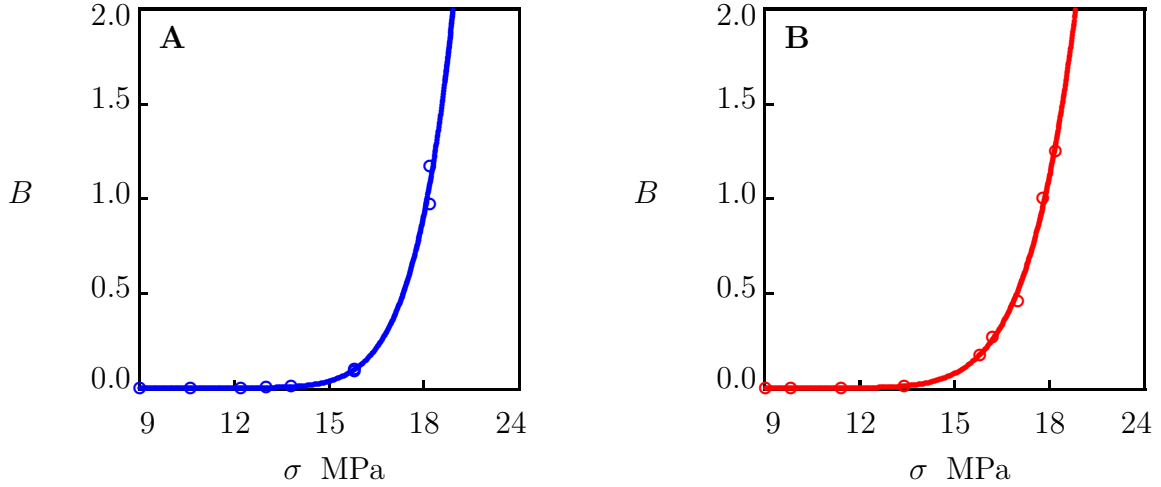


Figure 8: Parameter B versus tensile stress σ . Circles: treatment of experimental data on virgin (A) and recycled (B) HDPE. Solid lines: results of numerical analysis.

Figures 3 and 4 demonstrate good agreement between results of numerical analysis and the experimental creep diagrams along the intervals of primary and secondary creep. Slight deviations between the data and results of simulation are observed along the intervals of tertiary creep in Figures 4 and 5 only. These discrepancies arise because the model does not account for damage accumulation at the final stage of creep flow.

The coefficients α , A , and B for recycled HDPE are plotted versus tensile stress σ in Figures 6 to 8. For comparison, we present also the corresponding dependencies for virgin HDPE obtained in [20]. The data are approximated by Equations (12)–(14) with the adjustable parameters reported in Table 4. The coefficients α_0 , α_1 , A_1 and B_1 are calculated by the least-squares technique. The parameters m , n and a are determined by the nonlinear

regression method.

Table 4: Material parameters for virgin and recycled HDPE (creep tests with various stresses σ)

Coefficient α				
HDPE	α_0	α_1	σ_* MPa	m
Virgin	1.982	$8.08 \cdot 10^{-7}$	9.0	7.0
Recycled	0.0	$2.34 \cdot 10^{-3}$	9.2	4.0
Coefficient A				
HDPE	A_0	A_1	σ_* MPa	a MPa $^{-1}$
Virgin	$4.67 \cdot 10^{-2}$	$-3.90 \cdot 10^{-2}$	13.5	1.1
Recycled	$2.90 \cdot 10^{-2}$	$2.01 \cdot 10^{-2}$	16.0	4.0
Coefficient B				
HDPE	B_1	σ_* MPa	n	
Virgin	$3.51 \cdot 10^{-9}$	9.0	8.0	
Recycled	$1.28 \cdot 10^{-7}$	9.0	6.6	

Figures 6 and 8 demonstrate similar effects of tensile stress σ on the rates α and B of the viscoplastic flow in amorphous and crystalline regions. It should be noted, however, that the growth of α and B with σ is stronger (the quantities m and n are higher) in virgin HDPE compared with recycled HDPE.

Figure 7 shows a difference between the effects of stress σ on the coefficient A for virgin and recycled HDPE. The parameter A increases with σ in the virgin polymer and decreases with tensile stress in the recycled HDPE. However, the stress-induced changes in A are not substantial. This coefficient varies in the interval between 0.01 and 0.05 for virgin HDPE and in the interval between 0.03 and 0.05 for its recycled analog.

4.2 Validation of the model

To predict time to failure t_f of recycled HDPE in medium-term creep tests (with the duration of several days), we integrate Equations (8) and (9) with the parameters E , γ , Σ and κ reported in Table 3 and the parameters α , A and B determined by Equations (12)–(14) with the coefficients listed in Table 4. For each stress σ , evolution of tensile strain ϵ with time t is determined by Equation (7). Time to failure t_f is calculated from the condition

$$\epsilon(t_f) = \epsilon_*, \quad (15)$$

where the critical strain $\epsilon_* = 0.4$ is found from Figures 4 and 5 (it corresponds to transition to the tertiary creep in short-term creep tests). Equation (15) is based on the conventional assumption that the duration of the interval of tertiary creep is negligible compared with the durations of intervals of primary and secondary creep.

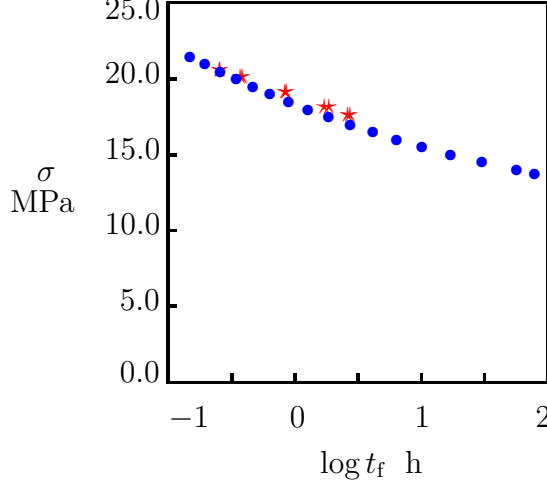


Figure 9: Tensile stress σ versus time-to-failure t_f for recycled HDPE under creep conditions. Asterisks: experimental data in creep tests with various stresses σ . Circles: predictions of the model.

Results of numerical analysis are reported in Figure 9 where the stress σ is plotted versus time to failure t_f . Results of simulation (circles) and presented together with the experimental data (asterisks) in creep tests with stresses $\sigma = 17.5, 18.0, 19.0, 20.0$ and 20.5 MPa (Figure 4). Figure 9 confirms the ability of the model to predict the stress-time to failure diagrams on recycled HDPE in medium-term creep tests.

4.3 Lifetimes of virgin and recycled HDPE

To compare the lifetimes of virgin and recycled HDPE under creep conditions, their times to failure t_f in long-term creep tests (with the duration up to 100 years) are calculated numerically. For this purpose, Equations (8) and (9) are integrated with the parameters E , γ , Σ and κ listed in Table 3 and the parameters α , A and B determined by Equations (12)–(14) with the coefficients collected in Table 4. For each polymer under consideration, time to failure t_f is found from condition (15).

Results of simulation are depicted in Figure 10 where tensile stress σ is plotted versus time-to failure t_f (d, m, and y stand for day, month and year, respectively). In this figure, circles denote results of numerical analysis, and solid lines provide their approximations by the power-law equation [37, 38]

$$\sigma = \sigma_0 + \sigma_1 \left(\frac{t_{f0}}{t_f} \right)^\delta \quad (16)$$

with the characteristic time $t_{f0} = 1$ h. The best-fit values of the material constants σ_0 , σ_1 and δ in Equation (16) are collected in Table 5.

Figure 10 provides the main result of this study. It shows that virgin and recycled HDPE with similar mechanical characteristics (the Young modulus, yield stress, and strain

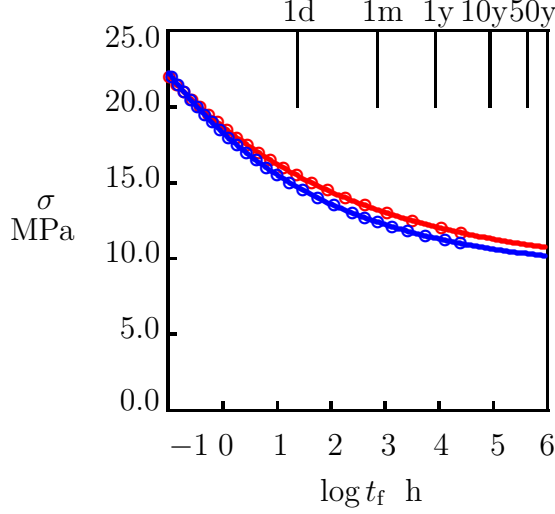


Figure 10: Tensile stress σ versus time-to-failure t_f under creep conditions. Circles: predictions of the model with $\epsilon_{cr} = 0.4$ for virgin (red) and recycled (blue) HDPE. Solid lines: approximation of the data by Equation (16).

at break) have practically identical lifetimes under tensile creep conditions. Unlike previous observations that revealed a pronounced decay in creep resistance when the same polymer was recycled [11, 12], our analysis shows that that creep resistance of the recycled material (prepared from post-consumer plastic waste of a different grade of HDPE) is similar to that of the virgin HDPE. Figure 10 demonstrates that specimens withstand 50 years of creep under tensile stresses lower than 10.9 and 10.3 MPa for virgin and recycled HDPE, respectively. Replacement of the virgin HDPE with its recycled analog leads to an insignificant reduction in the critical stress by 5.5% only. This may be explained by a higher stiffness of the recycled polymer (Table 3) and a less pronounced growth of the rates of viscoplastic flow in amorphous (Figure 6) and crystalline (Figure 8) regions.

Table 5: Material parameters for virgin and recycled HDPE (long-term creep tests with various stresses σ)

HDPE	σ_0 MPa	σ_1 MPa	δ
Virgin	9.609	9.108	0.129
Recycled	9.241	9.075	0.155

Although the above conclusion opens a new area of engineering applications for recycled polymers, it should be treated with caution. It is conventionally presumed that the stress–time to failure diagrams for polyethylene pipes consist of three intervals [39]. The model under consideration describes adequately the lifetime along the first interval (which corresponds to ductile failure of HDPE). The other intervals are associated with quasi-brittle failure driven by slow growth of micro-cracks and brittle failure caused by chemical degradation of this polymer [32]. Analysis of crack resistance of virgin and recycled HDPE under various loading programs will be conducted in a subsequent study.

5 Conclusions

Replacement of virgin polymers with their recycled analogs is attractive from the economical and environmental standpoints, but it is not always possible because of substantial deterioration of the mechanical properties of recyclates induced by their degradation during the service life and recycling process. Due to a pronounced reduction in resistance to creep, fatigue, and crack growth, recycled polymers cannot meet the same property profiles for long-term performance applications as their virgin counterparts.

To avoid a noticeable decline in mechanical characteristics of recycled materials, it was proposed in [18, 19] to replace a virgin polymer of a special grade with its recycled analog (a post-consumer recyclate prepared from another grade) whose properties after recycling (evaluated in tensile tests) are close to those of the virgin material. This approach opens a way for the use of recycled polymers in short-term application. However, its suitability for long-term applications has not yet been evaluated.

A thorough experimental investigation is performed of the mechanical response of virgin HDPE used for insulation of pipes for district heating and recycled HDPE manufactured from post-consumer household plastic waste. The Young's modulus, yield stress, and elongation to break of these two polymers adopt similar values (Table 1). Their viscoelastic and viscoplastic responses in short-term tensile relaxation and creep tests are adequately described by the same model presented in Section 3 (Figures 2 to 5). However, the material parameters of virgin and recycled HDPE determined by fitting experimental data in relaxation and creep tests differ noticeably (Tables 3 and 4).

The lifetime of virgin and recycled HDPE under creep conditions is evaluated by means of numerical simulation of the governing equations with the material parameters found by matching observations in short-term tests. Validation of the model is performed by comparison of its predictions with experimental data in short-term creep tests (Figure 9). The main result of the study is that the stress–time to failure diagrams for virgin and recycled HDPE practically coincide (Figure 10 and Table 5). Numerical analysis reveals that recycled HDPE withstands 50 years of creep under tensile stress which is lower by only 5.5% than that for virgin HDPE.

Acknowledgement

Financial support by Innovationsfonden (Innovation Fund Denmark, project 9091-00010B) is gratefully acknowledged.

References

- [1] Ignatyev, I.A.; Thielemans, W.; Vander Beke, B. Recycling of polymers: A review. *ChemSusChem* **2014**, *7*, 1579–1593.

- [2] Westlie, A.H.; Chen, E.Y.-X.; Holland, C.M.; Stahl, S.S.; Doyle, M.; Trenor, S.R.; Knauer, K.M. Polyolefin innovations toward circularity and sustainable alternatives. *Macromol. Rapid Commun.* **2022**, *43*, 2200492.
- [3] Law, K.L.; Narayan, R. Reducing environmental plastic pollution by designing polymer materials for managed end-of-life. *Nat. Rev. Mater.* **2022**, *7*, 104–116.
- [4] Thiounn, T.; Smith, R.C. Advances and approaches for chemical recycling of plastic waste. *J. Polym. Sci.* **2020**, *58*, 1347–1364.
- [5] Kartalis, C.N.; Papaspyrides, C.D.; Pfaendner, R.; Hoffmann, K.; Herbst, H. Mechanical recycling of postused high-density polyethylene crates using the restabilization technique. I. Influence of reprocessing. *J. Appl. Polym. Sci.* **1999**, *73*, 1775–1785.
- [6] Kartalis, C.N.; Papaspyrides, C.D.; Pfaendner, R.; Hoffmann, K.; Herbst, H. Mechanical recycling of post-used HDPE crates using the restabilization technique. II: influence of artificial weathering. *J. Appl. Polym. Sci.* **2000**, *77*, 1118–1127.
- [7] Vilaplana, F.; Karlsson, S. Quality concepts for the improved use of recycled polymeric materials: A review. *Macromol. Mater. Eng.* **2008**, *293*, 274–297.
- [8] Oblak, P.; Gonzalez-Gutierrez, J.; Zupancic, B.; Aulova, A.; Emri, I. Processability and mechanical properties of extensively recycled high density polyethylene. *Polym. Degrad. Stab.* **2015**, *114*, 133–145.
- [9] Cecon, V.S.; Da Silva, P.F.; Vorst, K.L.; Curtzwiler, G.W. The effect of post-consumer recycled polyethylene (PCRPE) on the properties of polyethylene blends of different densities. *Polym. Degrad. Stab.* **2021**, *190*, 109627.
- [10] Vidakis, N.; Petousis, M.; Maniadi, A. Sustainable additive manufacturing: Mechanical response of high-density polyethylene over multiple recycling processes. *Recycling* **2021**, *6*, 4.
- [11] Alzerreca, M.; Paris, M.; Boyron, O.; Orditz, D.; Louarn, G.; Correc, O. Mechanical properties and molecular structures of virgin and recycled HDPE polymers used in gravity sewer systems. *Polym. Testing* **2015**, *46*, 1–8.
- [12] Shaheen, E.T.; Sargand, S.M.; Masada, T.; Khoury, I. Long-term behavior prediction of HDPE containing postconsumer recycled material using stepped isostress method. *J. Mater. Civ. Eng.* **2022**, *34*, 04022261.
- [13] Zhang, J.; Hirschberg, V.; Rodrigue, D. Blending recycled high-density polyethylene HDPE (rHDPE) with virgin (vHDPE) as an effective approach to improve the mechanical properties. *Recycling* **2023**, *8*, 2.

- [14] Zhang, J.; Hirschberg, V.; Rodrigue, D. Mechanical fatigue of recycled and virgin high-/low-density polyethylene. *J. Appl. Polym. Sci.* **2023**, *140*, e53312.
- [15] Sciammarella, C.A.; Yang, Y. Slow crack growth in post-consumer recycled high-density polyethylene. *Mech. Time-Depend. Mater.* **2000**, *4*, 257–274.
- [16] Na, S.; Nguyen, L.; Spatari, S.; Hsuan, Y.G. Effects of recycled HDPE and nanoclay on stress cracking of HDPE by correlating J_c with slow crack growth. *Polym. Eng. Sci.* **2018**, *58*, 1471–1478.
- [17] Juan, R.; Dominguez, C.; Robledo, N.; Paredes, B.; Garcia-Munoz, R.A. Incorporation of recycled high-density polyethylene to polyethylene pipe grade resins to increase close-loop recycling and underpin the circular economy. *J. Clean. Prod.* **2020**, *276*, 124081.
- [18] Istrate, I.-R.; Juan, R.; Martin-Gamboa, M.; Dominguez, C.; Garcia-Munoz, R.A.; Dufour, J. Environmental life cycle assessment of the incorporation of recycled high-density polyethylene to polyethylene pipe grade resins. *J. Clean. Prod.* **2021**, *319*, 128580.
- [19] Juan, R.; Dominguez, C.; Robledo, N.; Paredes, B.; Galera, S.; Garcia-Munoz, R.A. Challenges and opportunities for recycled polyethylene fishing nets: Towards a circular economy. *Polymers* **2021**, *13*, 3155.
- [20] Drozdov, A.D.; Hoj Jermiin, R.; deClaville Christiansen, J. Lifetime predictions for high-density polyethylene under creep: experiments and modeling. *Polymers* **2023**, *15*, 334.
- [21] Nguyen, K.Q.; Cousin, P.; Mohamed, K.; Robert, M.; Benmokrane, B. Comparing short-term performance of corrugated HDPE pipe made with or without recycled resins for transportation infrastructure applications. *J. Mater. Civ. Eng.* **2022**, *34*, 04021427.
- [22] Brusselle-Dupend, N.; Cangemi, L. A two-phase model for the mechanical behaviour of semicrystalline polymers. Part I: large strains multiaxial validation on HDPE. *Mech. Mater.* **2008**, *40*, 743–760.
- [23] Hiss, R.; Hobeika, S.; Lynn, C.; Strobl, G. Network stretching, slip processes, and fragmentation of crystallites during uniaxial drawing of polyethylene and related copolymers. A comparative study. *Macromolecules*, **1999**, *32*, 4390–4403.
- [24] Galeski, A.; Bartczak, Z.; Argon, A.S.; Cohen, R.E. Morphological alterations during texture-producing plastic plane strain compression of high-density polyethylene. *Macromolecules* **1992**, *25*, 5705–5718.
- [25] Drozdov, A.D.; Gupta, R.K. Nonlinear viscoelasticity and viscoplasticity of isotactic polypropylene. *Int. J. Engng. Sci.* **2003**, *41*, 2335–2361.

- [26] Drozdov, A.D.; Christiansen, J.deC. Thermo-viscoelastic and viscoplastic behavior of high-density polyethylene. *Int. J. Solids Struct.* **2008**, *45*, 4274–4288.
- [27] Drozdov, A.D.; Klitkou, R.; Christiansen, J.deC. Cyclic viscoplasticity of semicrystalline polymers with finite deformations. *Mech. Mater.* **2013**, *56*, 53–64.
- [28] Tanaka, F.; Edwards, S.F. Viscoelastic properties of physically cross-linked networks. Transient network theory. *Macromolecules* **1992** *25*, 1516–1523.
- [29] Drozdov, A.D. Cyclic thermo-viscoplasticity of high density polyethylene. *Int. J. Solids Struct.* **2010**, *47*, 1592–1602.
- [30] Drozdov, A.D.; Christiansen, J.deC.; Klitkou, R.; Potarniche, C.G. Viscoelasticity and viscoplasticity of polypropylene/polyethylene blends. *Int. J. Solids Struct.* **2010**, *47*, 2498–2507.
- [31] Williams, S.J.; Bache, M.R.; Wilshire, B. Recent developments in analysis of high temperature creep and creep fracture behaviour. *Mater. Sci. Technol.* **2010**, *26*, 1332–1337.
- [32] Sattar, M.; Othman, A.R.; Kamaruddin, S.; Akhtar, M.; Khan, R. Limitations on the computational analysis of creep failure models: A review. *Eng. Fail. Anal.* **2022**, *134*, 105968.
- [33] Gulmine, J.V.; Janissek, P.R.; Heise, H.M.; Akcelrud, L. Degradation profile of polyethylene after artificial accelerated weathering. *Polym. Degrad. Stab.* **2003**, *79*, 385–397.
- [34] Hsueh, H.-C.; Kim, J.H.; Orski, S.; Fairbrother, A.; Jacobs, D.; Perry, L.; Hunston, D.; White, C.; Sung, L. Micro and macroscopic mechanical behaviors of high-density polyethylene under UV irradiation and temperature. *Polym. Degrad. Stab.* **2020**, *174*, 109098.
- [35] Pinheiro, L.A.; Chinelatto, M.A.; Canevarolo, S.V. The role of chain scission and chain branching in high density polyethylene during thermo-mechanical degradation. *Polym. Degrad. Stab.* **2004**, *86*, 445–453.
- [36] Frank, A.; Arbeiter, F.J.; Berger, I.J.; Hutar, P.; Nahlik, L.; Pinter, G. Fracture mechanics lifetime prediction of polyethylene pipes. *J. Pipeline Syst. Eng. Pract.* **2019**, *10*, 04018030.
- [37] Guedes, R.M. Lifetime predictions of polymer matrix composites under constant or monotonic load. *Composites A* **2006**, *37*, 703–715.

- [38] Bi, G.; Li, Z.; Wang, Q.; Jiang, D. An examination of creep failure criterion based on a strain threshold identified with a power law model. *Mech. Time-Depend. Mater.* **2022**, *26*, 195–209.
- [39] Zha, S.; Lan, H.-q.; Huang, H. Review on lifetime predictions of polyethylene pipes: Limitations and trends. *Int. J. Press. Vessel Pip.* **2022**, *198*, 104663.